Modern Physics Letters A
© World Scientific Publishing Company

IMPLEMENTATION OF THE ATLAS-SUSY-2018-32 ANALYSIS IN THE MADANALYSIS 5 FRAMEWORK

JACK Y. ARAZ

Institute for Particle Physics Phenomenology, Durham University, South Road, Durham, DH1 3LE, UK

jack.araz@durham.ac.uk

BENJAMIN FUKS

Laboratoire de Physique Théorique et Hautes Energies (LPTHE), UMR 7589, Sorbonne Université et CNRS, 4 place Jussieu, 75252 Paris Cedex 05, France

Institut Universitaire de France, 103 boulevard Saint-Michel, 75005 Paris, France

fuks@lpthe.jussieu.fr

Received (November 19, 2020)
Revised (Day Month Year)

We present the implementation in MadAnalysis 5 of the ATLAS-SUSY-2018-32 search for new physics, and document the validation of this re-implementation. This analysis targets, with 139 fb^{-1} of proton-proton collisions at a centre-of-mass energy of 13 TeV recorded by the ATLAS detector, the electroweak pair production of supersymmetric charginos and sleptons when they further decay into a final state comprising a pair of leptons and missing energy. The validation of our work is based on three R-parity conserving supersymmetric benchmark setups that feature, respectively, chargino pair-production followed by decays into leptons via an intermediate weak boson, chargino pair-production followed by chargino cascade decays into a leptons through a slepton mediator, and slepton pair-production followed by slepton direct decays into leptons.

1. Introduction

Supersymmetry (SUSY) is one of the most popular extensions of the Standard Model (SM). By naturally extending the Poincaré algebra and linking the fermionic and bosonic degrees of freedom of the theory, SUSY could provide, among others, a solution for the hierarchy problem of the SM and an explanation for the problematics of dark matter. The so-called Minimal Supersymmetric Standard Model (MSSM) [1,2] consists in the direct supersymmetrisation of the SM, giving thus rise to one SUSY partner to each SM degrees of freedom. In this framework, the slepton mass eigenstates are the superpartners of the SM leptons, and the electroweakino mass eigenstates consist of admixtures of the partners of the SM gauge and Higgs fields. More precisely, electroweakinos comprise the electrically-charged charginos

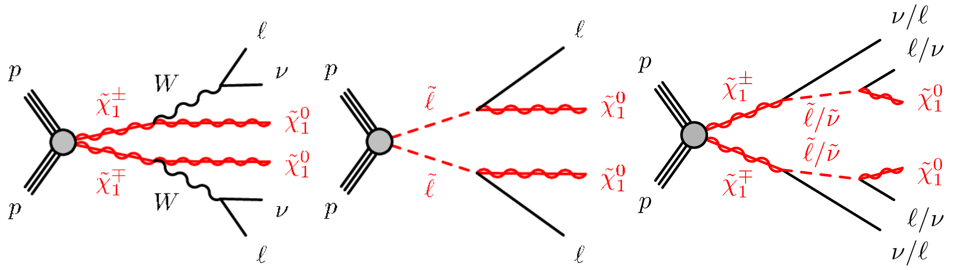

Fig. 1. Representative Feynman diagrams for the scenarios used for the validation of our reimplementation of the ATLAS-SUSY-2018-32 analysis. We consider chargino production followed by decays through electroweak bosons (left), slepton production followed by direct decays into leptons and missing energy (centre) and chargino production followed by decays mediated by an intermediate slepton or sneutrino (right). The diagrams have been taken from Ref. [3].

($\tilde{\chi}_i^{\pm}$, $i \in 1, 2$) and the electrically-neutral neutralinos ($\tilde{\chi}_i^0$, $i \in 1, 2, 3, 4$). The lightest neutralino is often considered to be the lightest supersymmetric particle (LSP), hence a potentially viable candidate for dark matter.

The ATLAS-SUSY-2018-32 analysis [3] has been structured to look for new physics signals that might appear due to charginos and sleptons. It searches for dilepton and missing energy final states which can emerge from the production of either a pair of lightest charginos, or of a pair of sleptons. Two separate benchmarks have been constructed for this purpose in the chargino case. First, a pure wino-like ($\tilde{W}$) chargino is considered to decay into a bino-like ($\tilde{B}$) LSP and a lepton via an intermediate W-boson. Second, the same wino-like chargino is assumed to cascade decay to the same final state, but this time through a slepton exchange. Additionally, a third benchmark scenario is dedicated to the pair production of sleptons that decay each into a lepton and an LSP. Those three cases are illustrated with the Feynman diagrams of Fig. 1.

Those three scenarios have been analysed to constrain the corresponding simplified models. The experimental results have shown that for a massless LSP, chargino masses up to 420 GeV are excluded at 95% confidence level (CL) in the first class of scenarios (chargino pair production and decay via a charged weak gauge boson). A more severe bound has been set on the second class of scenarios, when charginos decay through an intermediate slepton. The masses are in this case constrained to be larger than 1 TeV at 95% CL. Finally, slepton mass bounds, as derived in the context of the third class of scenarios, are of 700 GeV.

In the rest of this note, we present the recast of ATLAS-SUSY-2018-32 analysis of Ref. [3] in the MadAnalysis 5 framework, that is now available from the MadAnalysis 5 Public Analysis Database and the MadAnalysis 5 dataverse [4].

2. Description of the analysis

This analysis targets a signature made of two lepton and missing transverse energy, as could arise from the production and decay of a pair lightest charginos ($\tilde{\chi}_1^{\pm}$) or slepton ($\tilde{l}_i$). As mentioned in the previous section, the results are interpreted in three classes of simplified models depicted in the diagrams of Fig 1. The first two of these extend the SM by a chargino and a neutralino LSP, the difference between them lying at the level of the chargino decay. In the first setup, charginos decay into a single lepton and missing energy via an intermediate W-boson, whereas in the second setup, they decay via an intermediate slepton. In the last class of simplified models under consideration, the SM is supplemented by a charged slepton and a neutralino LSP, the slepton being taken directly decaying into the LSP and a lepton. The validation of our re-implementation is achieved in these three cases.

2.1. *Object definitions*

Jets are obtained by the clustering all participants to the hadronic activity in the event, electrons and photons according to the anti-k_T algorithm [5], as embedded in the FastJet package version 3.3.3 [6], with a radius parameter set to $R = 0.4$. Jet candidates are then extracted by requiring the reconstructed objects to have a minimum transverse momentum $p_T > 20$ GeV and a pseudorapidity satistying $|\eta| < 2.4$.

Electron and muons are required to satisfy strong isolation conditions to be considered as a signal leptons.

A signal electron is required to have a minimum p_T of 10 GeV and to be within $|\eta| < 2.47$. These electrons are then required to be isolated from the calorimetric activity and any other charged track. This is achieved in practice by constraining the sum of the p_T of all tracks lying in a cone of radius ΔR around the electron to be smaller than 15% of the electron transverse momentum, the cone radius being defined by $\Delta R = \min(10/p_T, 0.2)$. Moreover, the calorimetric activity I^e_{rel} in a cone of radius $\Delta R = 0.2$ around the electron is restricted to be smaller than 20% of the electron p_T. For very hard electrons with $p_T > 200$ GeV, a special isolation treatment is, however, implemented. In this case, one solely imposes the signal electron to be calorimetrically isolated, requiring $I^e_{rel} < \max(0.015 p_T, 3.5)$.

Signal muons are defined similarly. Their transverse momentum is imposed to fulfil $p_T > 10$ GeV and their pseudorapidity $|\eta| < 2.7$. Track-based isolation implies that the sum of the transverse momentum of all tracks lying in a cone of radius $\Delta R = \min(10/p_T, 0.3)$ around the muon is smaller than 15% of the muon transverse momentum, whilst calorimetric isolation enforces $I^\mu_{rel} < 0.3 p_T$, for a cone of radius $\Delta R = 0.2$ centred on the muon.

Finally, all jets at a distance in the transverse plane of $\Delta R \leq 0.2$ (0.4) of an electron (muon) are removed, and all electrons are required to be separated from any muon by least $\Delta R = 0.2$. The collection of b-jets is extracted from the collection of cleaned signal jets.

2.2. *Event selection*

The considered ATLAS-SUSY-2018-32 analysis includes four sets of signal regions differing by the properties of the dilepton system and the jet activity in the event. Two categories of signal regions feature a pair of leptons of different flavours (DF). Regions of the first class impose a veto to the presence of any final-state signal jet, whereas regions of the second sub-category allow for the presence of one jet in the final state. Similarly, two classes of regions are designed to probe final states featuring a pair of leptons of the same flavour (SF), these two sub-categories differing by requiring either zero or one final-state jet.

After dedicated pre-selection requirements, all signal regions are further divided into different bins in the m_{T2} observable defined by [7, 8]

$$m_{T2}(\mathbf{p}_{T,1}, \mathbf{p}_{T,2}, \mathbf{p}_T^{\rm miss}) = \min_{\mathbf{q}_{T,1}+\mathbf{q}_{T,2}=\mathbf{p}_T^{\rm miss}} \left\{\max\left[m_T(\mathbf{p}_{T,1}, \mathbf{q}_{T,1}), m_T(\mathbf{p}_{T,2}, \mathbf{q}_{T,2})\right]\right\} \ .$$

Here $\mathbf{p}_{T,1}$ and $\mathbf{p}_{T,2}$ are transverse momentum vectors of the two leptons and $\mathbf{q}_{T,1}$ and $\mathbf{q}_{T,2}$ are chosen to be a decomposition of the missing momentum vector, $\mathbf{q}_{T,1} + \mathbf{q}_{T,2} = \mathbf{p}_T^{\rm miss}$. A minimisation is performed over all possible decompositions of the missing momentum vector. For each decomposition, we calculate the transverse mass of the system constitued by the first (second) lepton and the $\mathbf{q}_{T,1}$ ($\mathbf{q}_{T,2}$) vector. The m_{T2} value is then taken as the minimum of the maximum of the two transverse masses associated with a given $\mathbf{p}_T^{\rm miss}$ decomposition.

In order to take trigger efficiencies into account, events are reweighed by 85% before any selection requirement. All signal regions then imposes that events feature two opposite-sign leptons with a minimum transverse momentum of 25 GeV, and whose invariant ,ass is larger than 25 GeV. A b-jet veto is further enforced. At this stage, the analysis is split into four categories, as mentioned above (DF/SF lepton pair, with or without one jet).

The DF signal regions additionally asks that the invariant mass of the lepton pair satisfies $m_{l_1,l_2} > 100$ GeV, whereas the SF ones increase this threshold to $m_{l_1,l_2} >$ 121.2 GeV. Finally, all signal regions require the presence of at least 100 GeV of missing transverse energy, and the missing energy significance, defined by $\slashed{E}_T/\sqrt{H_T}$, has to be larger than 10 $\sqrt{\rm GeV}$. In this expression, the denominator involves the H_T variable that consists of the scalar sum of the transverse momenta of all signal jets. A schematic representation of all signal regions is shown in Table 1.

3. Validation

3.1. *Event generation*

For the validation of the re-implementation of the ATLAS-SUSY-2018-32 analysis, we study the three different scenarios defined above. For the production of a pair of charginos that both decay via a W-boson, we choose a mass spectrum such that $m(\tilde\chi_1^\pm, \tilde\chi_1^0) = (300, 50)$ GeV, all other SUSY states being decoupled. Similarly, for the scenario focusing on slepton pair production, we choose

Table 1. Schematic representation of the ATLAS-SUSY-2018-32 signal region definitions.

Different Flavour (DF)		Same Flavour (SF)	
OS dilep. with $p_T^{l_1,l_2} > 25$ [GeV]			
$m_{l_1,l_2} > 25$ [GeV]			
b veto			
DF dilep. & $N_j = 0$	DF dilep. & $N_j = 1$	SF dilep. & $N_j = 0$	SF dilep. & $N_j = 1$
$m_{l_1,l_2} > 100$ [GeV]		$m_{l_1,l_2} > 121.2$ [GeV]	
$\not{E}_T > 110$ [GeV]			
$\not{E}_T$ Sig. > 10 [$\sqrt{\text{GeV}}$]			
m_{T2} bins			

$m(\tilde{l}^\pm, \tilde{\chi}_1^0) = (400, 200)$ GeV and decouple the rest of the spectrum. Finally, for the scenario where the two pair-produced charginos decay via an intermediate slepton, the mass spectrum is chosen to be $m(\tilde{\chi}_1^\pm, \tilde{l}^\pm, \tilde{\chi}_1^0) = (600, 300, 1)$ GeV, with again all other superpartners being decoupled. All SLHA spectrum files can be found in dedicated HEPData records provided by the ATLAS collaboration [9].

For our validation, we generate various leading-order event samples with MG5_aMC version 2.7.3 [10]. Following the MLM prescription [11], we merge samples featuring up to two extra jets at the matrix-element level, the merging scale being set to one quarter of the mass of the pair-produced SUSY particle. All events are showered and hadronised by means of Pythia 8 [12], and the simulation of the ATLAS detector is performed with the Delphes 3 package [13]. Through our simulation we used the leading-order set of NNPDF 2.3 parton distribution functions, as provided by LhaPDF [14,15]. Our re-implementation can then be used to investigate the ATLAS-SUSY-2018-32 sensitivity to the simulated signals, through MadAnalysis 5 version 1.8 (or more recent) [16]. All analysis files can be obtained from the MadAnalysis 5 Public Analysis Database [17].

3.2. *Comparison with the official results*

In this section we compare our productions for all the benchmarks described in section 3.1 with the corresponding official ATLAS results. To estimate the quality of our re-implementation, we define a variable δ to quantify the difference between the relative cut efficiencies as obtained from the ATLAS and MadAnalysis 5 results,

$$\delta_i = \frac{|\varepsilon_i^{\text{ATLAS}} - \varepsilon_i^{\text{MA5}}|}{\varepsilon_i^{\text{ATLAS}}} \ .$$

Here ε_i represents the relative cut efficiency which is defined as $\varepsilon_i = N_i/N_{i-1}$, N_i being number of surviving events after the i^{th} cut. The analysis will be considered as validated provided that all δ_i values are found to satisfy $\delta \lesssim 20\%$. In the present recast exercise, it should be noted that the lack of public information related to how the ATLAS collaboration has prepared its Monte Carlo production introduces a certain bias and makes the comparison complicated.

Finally, in order to evaluated the statistical power associated with our event generation procedure, we quantify the Monte Carlo uncertainty through a $\Delta_{\rm MC}$ quantity defined by

$$\Delta_{\rm MC} = \frac{N_n}{\sqrt{N_n^{\rm MC}}} \ ,$$

where $N_n^{\rm MC}$ is defined by the number of unweighted Monte Carlo events surviving the last cut. In our validation, we aim to remain a 10% Monte Carlo uncertainty, that is found to always be smaller than the magnitude of the deviation between the MadAnalysis 5 predsictions and the ATLAS results after the last cut.

Our results include a comparison between MadAnalysis 5 predictions and ATLAS official results for all four considered classes of signal regions, that respectively target the production of a SF lepton pair with 0 jet, the production of a SF lepton pair with 1 jet, the production of a DF lepton pair with 0-jet and the production of a DF lepton pair with 1 jet. As only ATLAS predictions for the $m_{T2} \in [100, \infty[$ GeV bin are available in HEPData, we accordingly restrict the discussion to this sole inclusive bin.

Tables 2 and 3 include cut-flow results for the benchmark simplified model featuring chargino production and decay via a W-boson. As can be seen in the lower panel of table 3, the largest variation from the ATLAS results has been observed to be 20.3% for the $\not{E}_T$ significance requirement. This disagreement stems from potentially genuine differences between the implementation of this cut in our reimplementation and in the non-public ATLAS code. However, our definition still gives a reasonably acceptable deviation from the ATLAS results, especially after accounting for all other cuts.

We then present results for slepton production (third class of benchmarks) in table 4, and for chargino pair-production followed by chargino decays via an intermediate slepton (second class of benchmarks) in tables 5 and 6.

All ten tables comprise two main columns, one for the ATLAS results and one for the MadAnalysis 5 ones. These columns are further divided, so that they include the number of events surviving each cut, the relative cut efficiencies and the δ_i quantities for each cut. All tables have been prepared with the `ma5_expert` package [18].

4. Conclusions

In this validation note, we presented our efforts on re-implementing the ATLAS-SUSY-2018-32 analysis in the MadAnalysis 5 framework. We have validated our work in the context of three simplified models dedicated to the production of electroweakinos and sleptons. The validation has been achieved by comparing predictions obtained with our code to official results from the ATLAS collaboration. We

Table 2. Cut-flow associated with the signal region dedicated to the production of a SF lepton pair without any jet (upper) or with a single jet (lower), for a benchmark scenario of the first category (production of a pair of charginos that decay each via a W-boson), for a spectrum defined by $m(\tilde{\chi}_1^{\pm}, \tilde{\chi}_1^0) = (300, 50)$ GeV.

	ATLAS		MadAnalysis 5		
	Events	ε	Events	ε	δ [%]
Initial	26432.0	-	26432.0	-	-
OS dilep. with $p_T^{l_1,l_2} > 25$ [GeV]	565.0	0.021	570.1	0.022	0.9
$m_{l_1,l_2} > 25$ [GeV]	559.0	0.989	564.0	0.989	0.0
b veto	526.0	0.941	557.7	0.989	5.1
SF dilep. & $N_j = 0$	138.7	0.264	134.0	0.240	8.9
$m_{l_1,l_2} > 121.2$ [GeV]	92.4	0.666	81.9	0.612	8.2
$\not{E}_T > 110$ [GeV]	47.1	0.510	42.4	0.518	1.5
$\not{E}_T$ Sig. > 10 [$\sqrt{\text{GeV}}$]	42.9	0.911	42.4	1.000	9.8
$m_{T2} \in [100, \infty[$ [GeV]	25.4	0.592	21.3	0.501	15.3
$\Delta_{\text{MC}}/N_{\text{yield}}$	4.3%		7.5%		

	ATLAS		MadAnalysis 5		
	Events	ε	Events	ε	δ [%]
Initial	26432.0	-	26432.0	-	-
OS dilep. with $p_T^{l_1,l_2} > 25$ [GeV]	565.0	0.021	570.1	0.022	0.9
$m_{l_1,l_2} > 25$ [GeV]	559.0	0.989	564.0	0.989	0.0
b veto	526.0	0.941	557.7	0.989	5.1
SF dilep. & $N_j = 1$	88.8	0.169	87.7	0.157	6.9
$m_{l_1,l_2} > 121.2$ [GeV]	58.9	0.663	57.5	0.656	1.1
$\not{E}_T > 110$ [GeV]	32.6	0.553	31.8	0.552	0.2
$\not{E}_T$ Sig. > 10 [$\sqrt{\text{GeV}}$]	26.9	0.825	30.5	0.961	16.4
$m_{T2} \in [100, \infty[$ [GeV]	14.0	0.520	13.9	0.455	12.6
$\Delta_{\text{MC}}/N_{\text{yield}}$	5.7%		9.4%		

have obtained a good agreement at each step of the analysis and for each of the four considered signal regions, the deviations being usually smaller than 10%. The largest discrepancies can be traced to difficulties in modelling the missing energy significance, which however yields a small impact when including the entire selection. The re-implementation is therefore considered as validated.

The MadAnalysis 5 C++ code is available from the MadAnalysis 5 dataverse (https://doi.org/10.14428/DVN/EA4S4D) [4]. The material relevant for the validation benchmarks has been obtained from HEPData [9].

Table 3. Same as in table 2 but for a pair of DF leptons produced without any jet (upper) and with one jet (lower).

	ATLAS		MadAnalysis 5		
	Events	ε	Events	ε	δ [%]
Initial	26432.0	-	26432.0	-	-
OS dilep. with $p_T^{l_1,l_2} > 25$ [GeV]	565.0	0.021	570.1	0.022	0.9
$m_{l_1,l_2} > 25$ [GeV]	559.0	0.989	564.0	0.989	0.0
b veto	526.0	0.941	557.7	0.989	5.1
DF dilep. & $N_j = 0$	122.7	0.233	137.0	0.246	5.3
$m_{l_1,l_2} > 100$ [GeV]	94.2	0.768	103.7	0.757	1.4
$\not{E}_T > 110$ [GeV]	46.5	0.494	52.2	0.503	1.9
$\not{E}_T$ Sig. > 10 [$\sqrt{\text{GeV}}$]	42.2	0.908	52.2	1.000	10.2
$m_{T2} \in [100, \infty[$ [GeV]	26.4	0.626	30.1	0.578	7.6
$\Delta_{\text{MC}}/N_{\text{yield}}$	4.2%		6.3%		

	ATLAS		MadAnalysis 5		
	Events	ε	Events	ε	δ [%]
Initial	26432.0	-	26432.0	-	-
OS dilep. with $p_T^{l_1,l_2} > 25$ [GeV]	565.0	0.021	570.1	0.022	0.9
$m_{l_1,l_2} > 25$ [GeV]	559.0	0.989	564.0	0.989	0.0
b veto	526.0	0.941	557.7	0.989	5.1
DF dilep. & $N_j = 1$	81.9	0.156	88.2	0.158	1.5
$m_{l_1,l_2} > 100$ [GeV]	62.3	0.761	65.0	0.738	3.0
$\not{E}_T > 110$ [GeV]	33.8	0.543	35.4	0.544	0.3
$\not{E}_T$ Sig. > 10 [$\sqrt{\text{GeV}}$]	27.2	0.805	34.3	0.968	20.3
$m_{T2} \in [100, \infty[$ [GeV]	15.3	0.562	15.9	0.464	17.6
$\Delta_{\text{MC}}/N_{\text{yield}}$	5.2%		8.8%		

Acknowledgments

JYA has received funding from the European Union's Horizon 2020 research and innovation programme as part of the Marie Sklodowska-Curie Innovative Training Network MCnetITN3 (grant agreement no. 722104).

References

1. H. P. Nilles, *Phys. Rept.* **110**, 1 (1984).
2. H. E. Haber and G. L. Kane, *Phys. Rept.* **117**, 75 (1985).
3. ATLAS Collaboration, G. Aad *et al.*, *Eur. Phys. J. C* **80**, 123 (2020), arXiv:1908.08215 [hep-ex].
4. B. Fuks and J. Y. Araz, *https://doi.org/10.14428/DVN/EA4S4D* (2020).
5. M. Cacciari, G. P. Salam and G. Soyez, *JHEP* **04**, 063 (2008), arXiv:0802.1189 [hep-ph].

Table 4. Same is in table 2 but for a benchmark scenario of the third category (production of a pair of sleptons decaying each into a lepton and the LSP), for a spectrum defined by $m(\tilde{l}^{\pm}, \tilde{\chi}_1^0) = (400, 200)$ GeV.

	ATLAS		MadAnalysis 5		
	Events	ε	Events	ε	δ [%]
Initial	503.0	-	503.0	-	-
OS dilep. with $p_T^{l_1,l_2} > 25$ [GeV]	316.0	0.628	322.2	0.641	2.0
$m_{l_1,l_2} > 25$ [GeV]	315.0	0.997	322.1	1.000	0.3
b veto	298.0	0.946	316.6	0.983	3.9
SF dilep. & $N_j = 0$	136.0	0.456	141.7	0.448	1.9
$m_{l_1,l_2} > 121.2$ [GeV]	123.5	0.908	129.8	0.916	0.8
$\not{E}_T > 110$ [GeV]	97.5	0.789	100.1	0.771	2.3
$\not{E}_T$ Sig. > 10 [$\sqrt{\text{GeV}}$]	88.5	0.908	100.1	1.000	10.2
$m_{T2} \in [100, \infty[$ [GeV]	75.1	0.849	81.1	0.811	4.5
$\Delta_{\text{MC}}/N_{\text{yield}}$	2.7%		0.8%		

	ATLAS		MadAnalysis 5		
	Events	ε	Events	ε	δ [%]
Initial	503.0	-	503.0	-	-
OS dilep. with $p_T^{l_1,l_2} > 25$ [GeV]	316.0	0.628	322.2	0.641	2.0
$m_{l_1,l_2} > 25$ [GeV]	315.0	0.997	322.1	1.000	0.3
b veto	298.0	0.946	316.6	0.983	3.9
SF dilep. & $N_j = 1$	99.2	0.333	102.7	0.324	2.5
$m_{l_1,l_2} > 121.2$ [GeV]	90.3	0.910	94.1	0.916	0.6
$\not{E}_T > 110$ [GeV]	71.8	0.795	74.3	0.790	0.6
$\not{E}_T$ Sig. > 10 [$\sqrt{\text{GeV}}$]	61.3	0.854	72.9	0.981	14.9
$m_{T2} \in [100, \infty[$ [GeV]	51.1	0.834	55.7	0.764	8.4
$\Delta_{\text{MC}}/N_{\text{yield}}$	3.7%		0.7%		

6. M. Cacciari, G. P. Salam and G. Soyez, *Eur. Phys. J. C* **72**, 1896 (2012), arXiv:1111.6097 [hep-ph].
7. C. Lester and D. Summers, *Phys. Lett. B* **463**, 99 (1999), arXiv:hep-ph/9906349.
8. H.-C. Cheng and Z. Han, *JHEP* **12**, 063 (2008), arXiv:0810.5178 [hep-ph].
9. ATLAS Collaboration, *10.17182/hepdata.89413* (2020).
10. J. Alwall, C. Duhr, B. Fuks, O. Mattelaer, D. G. Öztürk and C.-H. Shen, *Comput. Phys. Commun.* **197**, 312 (2015), arXiv:1402.1178 [hep-ph].
11. M. L. Mangano, M. Moretti, F. Piccinini and M. Treccani, *JHEP* **01**, 013 (2007), arXiv:hep-ph/0611129.
12. T. Sjöstrand, S. Ask, J. R. Christiansen, R. Corke, N. Desai, P. Ilten, S. Mrenna, S. Prestel, C. O. Rasmussen and P. Z. Skands, *Comput. Phys. Commun.* **191**, 159 (2015), arXiv:1410.3012 [hep-ph].
13. DELPHES 3 Collaboration, J. de Favereau, C. Delaere, P. Demin, A. Giammanco, V. Lemaître, A. Mertens and M. Selvaggi, *JHEP* **02**, 057 (2014), arXiv:1307.6346

Table 5. Same is in table 2 but for a benchmark scenario of the third category (production of a pair of charginos decaying each into a lepton and the LSP via an intermediate slepton), for a spectrum defined by $m(\tilde{\chi}_1^\pm, \tilde{l}^\pm, \tilde{\chi}_1^0) = (600, 300, 1)$ GeV.

	ATLAS		MadAnalysis 5		
	Events	ε	Events	ε	δ [%]
Initial	1320.0	-	1320.0	-	-
OS dilep. with $p_T^{l_1,l_2} > 25$ [GeV]	430.0	0.326	450.7	0.341	4.8
$m_{l_1,l_2} > 25$ [GeV]	429.0	0.998	449.9	0.998	0.1
b veto	401.0	0.935	441.5	0.981	5.0
SF dilep. & $N_j = 0$	89.8	0.224	93.4	0.212	5.5
$m_{l_1,l_2} > 121.2$ [GeV]	82.2	0.915	84.8	0.907	0.9
$\not{E}_T > 110$ [GeV]	68.7	0.836	72.6	0.857	2.6
$\not{E}_T$ Sig. > 10 [$\sqrt{\text{GeV}}$]	63.5	0.924	72.6	1.000	8.2
$m_{T2} \in [100, \infty[$ [GeV]	56.0	0.882	59.1	0.814	7.7
$\Delta_{\text{MC}}/N_{\text{yield}}$	4.6%		1.2%		

	ATLAS		MadAnalysis 5		
	Events	ε	Events	ε	δ [%]
Initial	1320.0	-	1320.0	-	-
OS dilep. with $p_T^{l_1,l_2} > 25$ [GeV]	430.0	0.326	450.7	0.341	4.8
$m_{l_1,l_2} > 25$ [GeV]	429.0	0.998	449.9	0.998	0.1
b veto	401.0	0.935	441.5	0.981	5.0
SF dilep. & $N_j = 1$	74.0	0.185	73.5	0.166	9.8
$m_{l_1,l_2} > 121.2$ [GeV]	65.5	0.885	66.8	0.909	2.7
$\not{E}_T > 110$ [GeV]	55.9	0.853	57.6	0.863	1.1
$\not{E}_T$ Sig. > 10 [$\sqrt{\text{GeV}}$]	49.7	0.889	56.7	0.984	10.6
$m_{T2} \in [100, \infty[$ [GeV]	41.7	0.839	44.4	0.783	6.6
$\Delta_{\text{MC}}/N_{\text{yield}}$	5.3%		1.4%		

[hep-ex].
14. NNPDF Collaboration, R. D. Ball, V. Bertone, S. Carrazza, L. Del Debbio, S. Forte, A. Guffanti, N. P. Hartland and J. Rojo, *Nucl. Phys. B* **877**, 290 (2013), arXiv:1308.0598 [hep-ph].
15. A. Buckley, J. Ferrando, S. Lloyd, K. Nordström, B. Page, M. Rüfenacht, M. Schönherr and G. Watt, *Eur. Phys. J. C* **75**, 132 (2015), arXiv:1412.7420 [hep-ph].
16. E. Conte and B. Fuks, *Int. J. Mod. Phys. A* **33**, 1830027 (2018), arXiv:1808.00480 [hep-ph].
17. B. Dumont, B. Fuks, S. Kraml, S. Bein, G. Chalons, E. Conte, S. Kulkarni, D. Sengupta and C. Wymant, *Eur. Phys. J. C* **75**, 56 (2015), arXiv:1407.3278 [hep-ph].
18. J. Y. Araz, *https://github.com/jackaraz/ma5_expert* (2020).

Table 6. Same as in table 5 but for a pair of DF leptons produced without any jet (upper) and with one jet (lower).

	ATLAS		MadAnalysis 5		
	Events	ε	Events	ε	δ [%]
Initial	1320.0	-	1320.0	-	-
OS dilep. with $p_T^{l_1,l_2} > 25$ [GeV]	430.0	0.326	450.7	0.341	4.8
$m_{l_1,l_2} > 25$ [GeV]	429.0	0.998	449.9	0.998	0.1
b veto	401.0	0.935	441.5	0.981	5.0
DF dilep. & $N_j = 0$	82.8	0.206	92.8	0.210	1.8
$m_{l_1,l_2} > 100$ [GeV]	77.8	0.940	86.8	0.935	0.5
$\not{E}_T > 110$ [GeV]	66.8	0.859	73.8	0.850	1.0
$\not{E}_T$ Sig. > 10 [$\sqrt{\text{GeV}}$]	62.9	0.942	73.8	1.000	6.2
$m_{T2} \in [100, \infty[$ [GeV]	53.8	0.855	60.3	0.817	4.5
$\Delta_{\text{MC}}/N_{\text{yield}}$	4.8%		1.2%		

	ATLAS		MadAnalysis 5		
	Events	ε	Events	ε	δ [%]
Initial	1320.0	-	1320.0	-	-
OS dilep. with $p_T^{l_1,l_2} > 25$ [GeV]	430.0	0.326	450.7	0.341	4.8
$m_{l_1,l_2} > 25$ [GeV]	429.0	0.998	449.9	0.998	0.1
b veto	401.0	0.935	441.5	0.981	5.0
DF dilep. & $N_j = 1$	66.3	0.165	72.7	0.165	0.4
$m_{l_1,l_2} > 100$ [GeV]	61.3	0.925	68.4	0.941	1.8
$\not{E}_T > 110$ [GeV]	53.4	0.871	59.0	0.863	1.0
$\not{E}_T$ Sig. > 10 [$\sqrt{\text{GeV}}$]	48.6	0.910	58.0	0.984	8.1
$m_{T2} \in [100, \infty[$ [GeV]	40.7	0.837	45.7	0.788	5.9
$\Delta_{\text{MC}}/N_{\text{yield}}$	5.4%		1.3%		